Modeling and Simulation of Multi-walled Carbon Nanotubes using Molecular Dynamics Simulation

C. H. Wong[*,**], K. M. Liew[*,**], X. Q. He[*], M. J. Tan[**] and S. A. Meguid[***]

[*]Nanyang Centre for Supercomputing and Visualisation, Nanyang Technological University, Nanyang Avenue, Singapore 639798

[**]School of Mechanical and Production Engineering, Nanyang Technological University, Nanyang Avenue, Singapore 639798, mkmliew@ntu.edu.sg

[**]Engineering Mechanics and Design Laboratory, Department of Mechanical and Industrial Engineering, University of Toronto, 5 King's College Road, Toronto, Ontario, M5S 3G8, Canada

ABSTRACT

Molecular dynamics simulation is performed on the buckling behavior of single and multi-walled carbon nanotubes under axial compression. Brenner's 'second generation' empirical potential is used to describe the many-body short range interatomic interactions for single-walled carbon nanotubes, while the Lennard Jones 12-6 model for van der Waals potential is added for multi-walled carbon nanotubes to describe the interlayer interactions. Results indicate that there exists an optimum diameter for single-walled nanotubes at which the buckling load P_{cr} reaches its maximum value. The buckling load P_{cr} for single-walled nanotube increases rapidly with the increase of the diameter d up to the optimum diameter. However, any further increase in the diameter d after the optimum diameter will result in a slow decline in buckling load P_{cr} until a steady value is reached. The buckling behavior of multi-walled nanotubes is also presented The effects of layers on the buckling load of multi-walled nanotubes are examined.

Keywords: carbon nanotube, molecular dynamics, buckling, nanomechanics, simulation

1 INTRODUCTION

The discovery of carbon nanotubes in the early 1990s by Iijima [1] has sparked a revolution in chemical physics and materials science in recent years. Since then, much research has been done on these new forms of carbon due to its exceptional mechanical properties. Among these research, computer simulations using empirical pair potentials, such as Brenner's 'second generation' empirical potential [2], are effective methods for the analysis of structural and mechanical properties carbon nanotubes.

In this paper, classical molecular dynamic simulations employing Brenner's 'second-generation' empirical potential function have been carried out for the buckling behavior of perfectly structured single and multi-walled carbon nanotubes under compressive deformation. Spontaneous plastic collapse of the nanotubes are described, which is in qualitative agreement with the experimental observations of Lourie *et al*. [3] and the simulated observations of Srivastava *et al*. [4] using the quantum generalized tight binding molecular scheme. From these buckling analyses, which are detailed in the following sections, the mechanical properties such as the buckling loads of the nanotubes can be determined.

2 NUMERICAL SIMULATION AND DISCUSSION

Using the Brenner's 'second generation' reactive empirical many-body bond order potential energy expression [2], which is computed as

$$E_{POT} \quad _{i\ j\ i} V^R\ r_{ij} \quad \bar{b}_{ij} V^A\ r_{ij} \quad , \tag{1}$$

the buckling behavior of single-walled and multi-walled carbon nanotubes are simulated by solving the equations of motions using the Gear's predictor-corrector algorithm.[22] The distance between atoms i and j are denoted by r_{ij}, the pair additive repulsive and attractive interactions are represented by V^R and V^A respectively, and the reactive bond order is expressed by $\bar{b}_{ij}$. The axial compression of perfectly structured single and multi-walled carbon nanotube is achieved by applying a rate of 20 m/s and 10 m/s respectively at both ends. At the same time, the atoms at both ends of the nanotube are kept transparent to the interatomic forces. The end atoms are then moved inwardly along the axis by small steps, followed by a conjugate gradient minimization method while keeping the end atoms fixed.

2.1 Single-walled Carbon Nanotubes

To characterize the buckling behavior of single-walled carbon nanotubes, a (8,0) single-walled carbon nanotube is used in the simulation. The nanotube has a length l 43 Å and diameter d 6.3 Å. Each time step used in this simulation is equivalent to 1 fs and the simulations were allowed to run for 20,000 time steps.

Figure 1 shows the plot of strain energy per atom, which is determined as the difference in total energy per atom of the strained and unstrained carbon nanotube, against strain, which is defined as the ratio of elongation/original length for the (8,0) carbon nanotubes after it is compressed axially using the Brenner's 'second generation' empirical potential function [2].

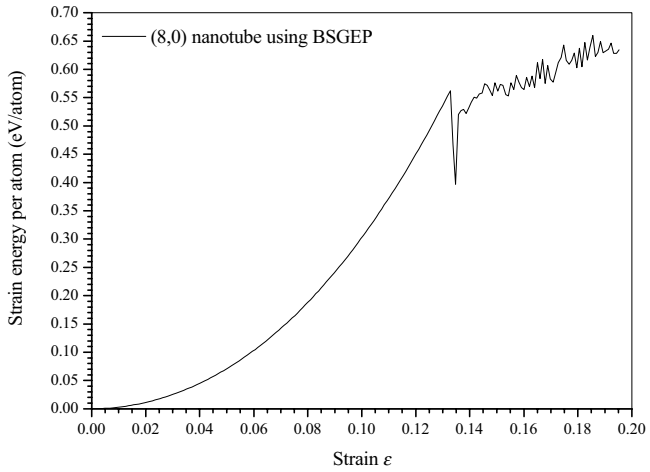

Figure 1: Computed strain energy per atom for (8,0) single-walled carbon nanotubes using Brenner's 'second generation' empirical potential (BSGEP) [2].

The (8,0) single-walled carbon nanotube undergoes elastic deformation before collapsing catastrophically at a certain critical strain of ε 0.13, resulting in a 30% spontaneous drop of strain energy per atom to 0.4 eV/atom. The nature of the spontaneous plastic collapse of single-walled nanotubes reported in this paper is in qualitative agreement with the experimental observation of Lourie *et al*. [3] and the simulated observation of Srivastava *et al*. [4] using the GTBMD scheme. The calculated critical stress σ_{cr} 149 GPa for the (8,0) single-walled carbon nanotube in this work is also close to the simulation work of Srivastava *et al*. [4] who obtained σ_{cr} 153 GPa. The (8,0) carbon nanotube is subjected to acute morphological changes, hence, higher strains are found in the (8,0) carbon nanotube, particularly around the kinks.

A length/diameter (l/d) ratio of 7.7:1 is used to illustrate the relationship between the diameters d and the buckling loads P_{cr} of selected zig-zag single-walled carbon nanotubes. From Fig. 2, it shows that as the diameter d of the zig-zag nanotube increases, there is a rapid increase in its buckling load P_{cr}. However, as the diameter d reaches an optimum value d 11.76 Å, any further increment beyond that will cause the buckling load P_{cr} to decrease slowly to a steady value of about 1.10 10^{-7} N. It is evident that the length l of the carbon nanotubes will affect the critical strain ε_{cr}.

It is worthy to note that the classical shell theory can be used for local buckling analysis of nanotubes. For a layer of cylindrical shell with length l, radius r, thickness t, the Young's modulus E, the Poisson's ratio ν, and m and $2n$ longitudinal and circumferential wave numbers, the critical stress for the buckling of the cylindrical shell is obtained as[23]

$$\sigma_{cr} \quad \frac{Et^3}{12\,1\quad \nu^2} \quad \frac{n^2 \quad \frac{m^2\pi^2r^2}{l^2}}{r^2 \quad \frac{m^2\pi^2r^2}{l^2}}^2 \quad \frac{E \quad \frac{m^2\pi^2r^2}{l^2}}{n^2 \quad \frac{m^2\pi^2r^2}{l^2}}^2 \quad (2)$$

In predicting the buckling load of nanotubes by using cylindrical shell model, almost all previous literatures adopted the interlayer separation of graphite, i.e. t = 3.4 Å as the representative thickness of single-walled nanotubes. However, the buckling loads obtained from Eq. (2) are larger than our molecular dynamics simulated results if t = 3.4 Å is used. Here, we take the diameter of carbon atom (1.54 Å) as the thickness of the nanotube. The Young's modulus E = 1.28 TPa is directly extracted from the experiment result by Wong *et al*. [5] for the calculation of buckling loads using Eq. (2). As the buckling load is not sensitive to the value of Poisson's ratio, it is taken as ν = 0.25. Using the cylindrical shell formula in Eq. (2) and molecular dynamics, buckling loads are computed for various zig-zig single-walled nanotubes, as shown in Fig. 2.

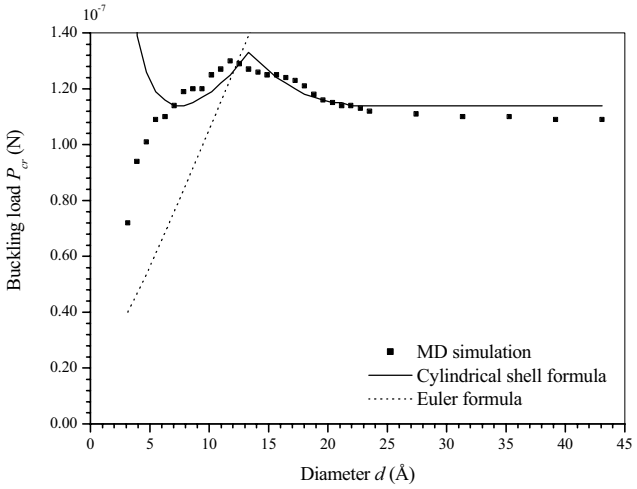

Figure 2: Comparison between cylindrical shell formula and molecular dynamics simulation for buckling loads P_{cr} of various zig-zig single-walled nanotubes with different diameters

It is observed from Fig. 2 that the two sets of results are in good agreement with diameter d ranging from 5.49 Å to 43.1 Å or larger. In spite of this, the results obtained from the cylindrical shell formula [Eq. (2)] for diameters d smaller than 4.7 Å do not agree well with that of the molecular dynamics simulation. This is because the nanotube behaves more like a rod than a cylindrical shell with thickness/radius (t/r) ratio larger than 0.66. In view

of this, the buckling loads of zig-zag nanotubes with fixed ends are also calculated using Euler's formula [6] and are presented in Fig. 2,

$$P_{cr} \quad \frac{4\pi^2 EI}{l^2}, \tag{3}$$

where I is the moment of inertia. For the fixed length/diameter (l/d) ratio, the buckling loads obtained from Euler's formula for nanotubes with fixed ends are proportional to the diameter d of nanotubes, as shown in Fig. 2, and is obvious from the trend that the Euler's formula is more reasonable than the cylindrical shell model in the estimation of the buckling loads of nanotubes with (t/r) ratio larger than 0.66.

2.2 Multi-walled Carbon Nanotubes

Comparisons are also made between various multi-walled carbon nanotubes to determine the effect of the number of layers on the properties of the multi-walled nanotubes. Three configurations of multi-walled nanotubes are considered in the simulation: the first is a two-walled (5,5) and (10,10) nanotube; the second is a three-walled (5,5), (10,10), and (15,15) nanotube; and the last is a four-walled (5,5), (10,10), (15,15), and (20,20) nanotube. The lengths of all three multi-walled nanotubes are $l \quad 60$ Å. And their diameters d are 13.52 Å, 20.36 Å, and 27.15 Å for the two, three and four layers multi-walled nanotubes respectively. In these simulations, the long-range van der Waals potential is added into the short-range covalent potential for the interlayer interaction using Lennard-Jones 12-6 potential [7]

$$V_{ij}\ r_{ij} \quad 4\frac{\xi}{\sigma}\ \frac{\sigma}{r_{ij}}^{12}\ \ \frac{\sigma}{r_{ij}}^{6}. \tag{4}$$

where coefficients of well-depth energy ξ and the equilibrium distance σ are 4.2038 10^{-3} eV and 3.4 Å, respectively [8].

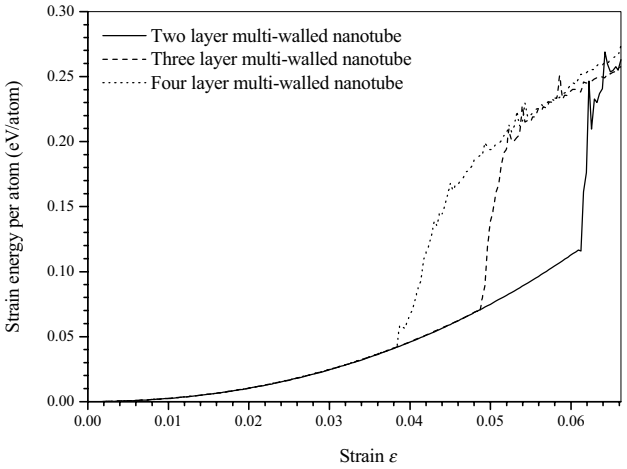

Figure 3: Strain energy per atom for two-walled, three-walled, and four-walled carbon nanotubes.

The van der Waals potential is nonzero only after the covalent potential is zero, such that there is no artificial reaction barrier formed by the steep repulsive wall of the Lennard-Jones 12-6 potential to prevent non-bonded atoms from chemical reaction.

The three multi-walled nanotubes are compressed axially using the same method as the single-walled nanotubes. Each time step is equivalent to 1 fs and there are a total of 20,000 time steps, which corresponds approximately to $\varepsilon \quad 0.066$.

Figure 3 depicts that the two-walled carbon nanotube manages to keep its elasticity for the longest with the largest critical strain at $\varepsilon \quad 0.06$, while the four-walled carbon nanotube has the lowest critical strain at $\varepsilon \quad 0.038$. Instead of a spontaneous decrease of strain energy upon buckling as evidenced in single-walled carbon nanotubes, the strain energy per atom increases until all the layers in the multi-walled carbon nanotubes are fully buckled.

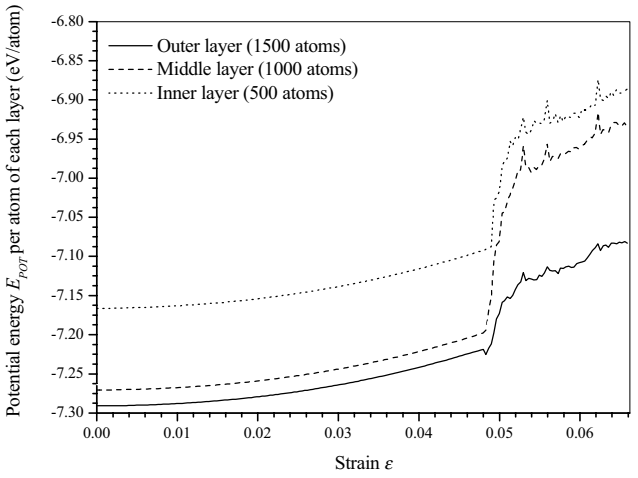

Figure 4: Potential energy per atom for each layer for (5,5), (10,10) and (15,15) three-walled carbon nanotube with diameter 20.36 Å.

The sudden increase in strain energy per atom for each layer is due to the spontaneous increase in potential energy of each atom for each layer as shown in Fig. 4. From the plot, it is observed that the middle layer has the largest increment of potential energy of each atom for each layer followed by the inner layer and then the outer layer. Being sandwiched between the outer and inner layer, when the three-walled carbon nanotube starts to buckle, the atoms at the middle layer will form more nearest-neighbors than those of the outer and inner layer. This causes the formation of sp^2 to sp^3 configuration, which leads to a larger increase in the empirical bond order function and consequently the potential energy.

Figure 5 shows the three-dimensional and cross-sectional three-walled nanotube at different strains. It is evident from Fig. 5(a) that the outer layer starts to deform first into a ring pattern at $\varepsilon \quad 0.0484$, while the middle and

inner layers are undeformed and their strain energies remain low. However, further compression at ε 0.0486 causes the middle layer to deform too, resulting in a sudden increase in the strain energy per atom because of the increase in potential energy due to the atoms in the middle layer. Similarly at this time, the inner layer maintains the elasticity of the nanotube temporarily as shortly after at ε 0.0493, the inner layer also starts to buckle, therefore increasing the overall potential energy and hence increasing the strain energy per atom further. After ε 0.052, all the layers are deformed, hence there is no further abrupt increase in potential energy due to sudden addition of nearest-neighbors.

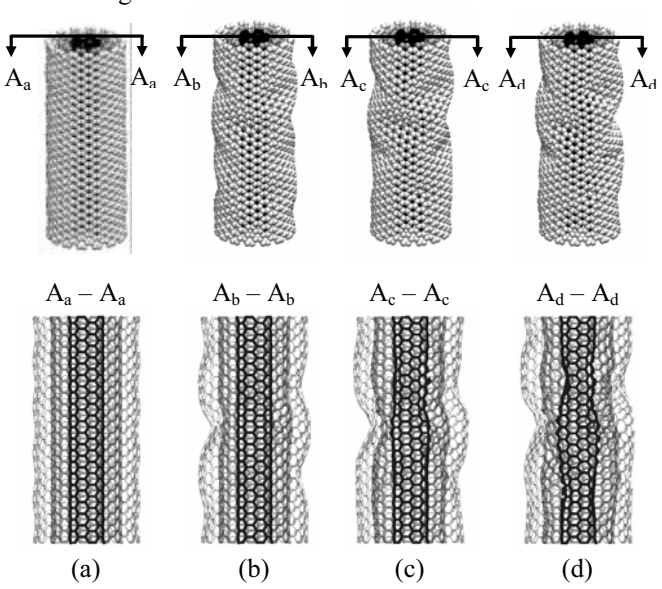

Figure 5: Three-dimensional and cross-sectional view of morphological changes for three-walled (5,5), (10,10), and (15,15) carbon nanotube with diameter 20.4 Å.

The buckling loads P_{cr} for two and three-walled carbon nanotubes are tabulated in Table 1. It is observed from the table that generally multi-walled carbon nanotubes have larger buckling loads P_{cr}. For instance, the (10,10), (15,15) two-walled carbon nanotube has a higher buckling load P_{cr} 2.02 10^{7} N compared to the (5,5), (10,10) two-walled carbon nanotube that has a buckling load P_{cr} 1.72 10^{7} N (see Table 1).

Two-walled		Three-walled	
$(n_1,m_1)(n_2,m_2)$	P_{cr} (10^{7} N)	$(n_1,m_1)(n_2,m_2)(n_3,m_3)$	P_{cr} (10^{7} N)
(5,5)(10,10)	1.72	(5,5)(10,10)(15,15)	2.46
(10,10)(15,15)	2.02	(10,10)(15,15)(20,20)	2.73
(15,15)(20,20)	2.09	(15,15)(20,20)(25,25)	2.81
(20,20)(25,25)	2.10	(20,20)(25,25)(30,30)	3.05

Table 1: Buckling loads for selected two and three-walled carbon nanotubes.

Moreover, Table 1 also verifies that as the number of layers in a carbon nanotube increases, its buckling load P_{cr} increases too. According to Table I, the buckling load P_{cr} for a (5,5) single-walled carbon nanotube is 0.88 10^{7} N, however if an extra outer layer is added to form a (5,5), (10,10) two-walled carbon nanotube, its buckling load P_{cr} will increase to 1.72 10^{7} N as seen in Table II. If another layer is further added to form a (5,5), (10,10), and (15,15) three-walled carbon nanotube, the buckling load P_{cr} will rise to 2.46 10^{7} N.

3 CONCLUSIONS

In conclusion, molecular dynamics simulation was used to analyze the structural properties of single and multi-walled nanotubes. The buckling loads for many single and multi-walled carbon nanotubes are determined in the study. The calculation shows that as the diameter of single-walled nanotubes increases, the buckling load P_{cr} increases rapidly up to the optimum buckling load P_{cr}. Any further increase beyond the optimum diameter d, however, will result in a slow decline in buckling load P_{cr} up to a steady value. Therefore, each single-walled carbon nanotubes has an optimum diameter d that yields the highest buckling load P_{cr}. In addition, the number of layers in a multi-walled nanotube will also affect its structural properties. When a single-walled carbon nanotube buckles, there is a sudden decrease in strain energy; however, when a multi-walled carbon nanotube buckles, there is a spontaneous increase in strain energy. This is due to the growth of potential energy as more chemical bonds change from sp^2 to sp^3 configuration.

REFERENCES

[1] Iijima, Nature (London) 354, 56, 1991.
[2] Brenner, Shenderova, Harrison, et al, J. of Phys: Cond Matt 14, 783, 2002.
[3] Lourie, Cox, and Wagner, Phys. Rev. Lett. 81, 1638, 1998.
[4] Srivastava, Menon, and Cho, Phys. Rev. Lett. 83, 2973, 1999.
[5] Wong, Sheehan, and Lieber, Science 277, 1971, 1997.
[6] Timoshenko and Gere, Van Nostrand Reinhold Company, USA, Chapt. 10, 1973.
[7] Lennard-Jones, Proc. Roy. Soc., London 106A, 441, 1924.
[8] Moller, Tildesley, Kim, and Quirke, J. Chem. Phys. 94, 8390, 1991.